PROCESS SIMULATION OF TIG WELDING FOR THE DEVELOPMENT OF AN AUTOMATIC ROBOT TORCH THROUGH HEAT PIPE – HEAD COOLING SYSTEM

K. ALALUSS* and P. MAYR**

*Steinbeis Innovation Centre Intelligent Functional Materials, Welding and Joining Techniques, Implementation, 01099 Dresden – Germany, e-mail: khaled.alaluss@stw.de
** Institute of Joining and Assembly Chemnitz University of Technology, 09126 Chemnitz – Germany , e-mail: schweisstech@mb.tu-chemnitz.de

DOI 10.3217/978-3-85125-615-4-49

ABSTRACT

Modern robot welding torches for arc welding are equipped with interchangeable neck systems. Generally, in TIG welding torches, the transfer powers to the electrode and the heat dissipation from the electrode occur just through the clamping area. The clamping geometry is usually formed in a ring. Therefore, a high resistance is generated between electrode and clamping system. This system suffers from power losses as well as limited heat dissipation. Furthermore, with this system, torch head setting needs tools and consumes a relatively long time. By developing of a non-linear thermo-flow-mechanical / magneto-hydro-dynamic (MHD) FE-model, using CFX ANSYS program, a novel robotic-TIG welding torch with an interchangeable head system and heat dissipation (heat pipe) was innovated. Depending on the predefined process parameters, the resulting thermo-physical heat output effects the torch-head design were investigated and analyzed then taken into account in the design process. The influences of the welding parameters such as current, shielding gas quantity on the torch design were determined through FE calculations. This determination process was connected to the design of the torch cooling system (heat pipe). The temperature distribution and its behavior at arc contour, shielding gas nozzle, and heat pipe body within the heat output range was determined. As well as, the distribution of flow gas velocity through the arc region and its behavior within the heat output range was determined. The use of a four heat pipes cooling system is sufficient for the maximum predefined power. The designed gas supply channels system gives efficient, functioning, and error-free gas flow results during the welding process. At maximum power range, the maximum calculated temperature at the shielding gas nozzle and at heat pipe – (tube body) is ≤ 350 K. Furthermore, the simulation results show the effect of arc focusing due to the shielding gas flow as well as the effect of increasing the welding current on the arc dynamics and their geometric shape. The performed simulation process shows a good alignment between the calculations and the experiments. Finally, a robotic TIG torch with high-quality performance and easy interchangeable torch's component was innovated and constructed, as well as high weld quality was achieved.

Keywords: Automatic TIG robot welding torch, Process simulation, Heat pipe cooling,

LIST OF SYMBOLS

B	[T = V s m^{-2}]	electromagnetic field
c	[J kg^{-1} K^{-1}]	heat capacity
D_a	[m^2 s^{-1}]	ambipolar diffusion coefficient
D_e	[m^2 s^{-1}]	electron diffusion coefficient
e n	[1 C = 1 A s]	electron flux
FE	-	finite-element
f_s	[N]	single forces in arc region
f_L	[N]	Lorentz force
J	[A m^{-2}]	electric current density
h	[J kg^{-1}]	specific enthalpy
N_e	[m^{-3}]	electron number density
N_0	[m^{-3}]	neutral atom density number
p	[Pa]	pressure
q	[J mm^{-2} s^{-1}]	heat flux
Q	[J s^{-1}]	thermal energy
S	[V]	electric potential
S_{Hc}	[J]	energy value at the cathode
S_{He}	[m^{-3}]	emitting electrons
S_{Hi}	[J = C kg^{-1}]	impact of ions
S_{RH}	[Ω]	resistive heating
T	[K]	temperature
α	[W m^{-2} K^{-1}]	heat transfer coefficient
η	[m^{-2} s^{-1}]	diffusion coefficient
$\dot{V}_{Shielding\ gas}$	[l min^{-1}]	shielding gas flow
$\dot{m}$	[l min^{-1}]	mass flow rate
ε	[W m^{-3} sr]	emission coefficient
γ_e	[S m^{-1}]	electrical conductivity
λ	[W m^{-1} K^{-1}]	thermal conductivity
λ_m	[m]	diffusion length
μ_0	[T m A^{-1}]	magnetic permeability
ν	[m s^{-1}]	velocity
η	[N s m^{-2}]	dynamic viscosity
Φ	[J C^{-1}]	electron diffusion
ϕ	[V]	electric current potential
ρ	[kg m^{-3}]	density
ω	[m s^{-1}]	electron drift

INTRODUCTION

Modern automatic robot welding torches for arc welding are equipped with interchangeable neck systems. Nowadays, in TIG welding torches, the tungsten electrodes are inserted from the back of the torch to fix it annularly in a clamping sleeve using a collet system. The

current transfer to the electrode while the heat dissipation from the electrode takes place exclusively via the clamping point. The geometry of the clamping system is designed as a clamping ring. This causes a high resistance between electrode and clamping system. This leads to a loss of power and lowering of the heat dissipation. Furthermore, with this clamping system, electrode distance to the component cannot be set without tools, and the torch head adjustment is very time-consuming. The exchange systems that are used for automatic/robot-TIG welding torches are constructed in the following technical versions: Short head design with tungsten electrode in "stick form"; and the long design (similar to hand torches) with long tungsten electrodes [1-3].

In the robotic TIG welding process, to achieve an exact arc positioning at the specific welding location, technical specifications are provided to the torch head and its changing system. These are constant heat dissipation in the torch head area, rapid replacement of wear parts, especially the cathode, reproducible replacement of the welding torch heads and rapid coupling of the process media (welding current, shielding gas and torch cooling system). The aim of this work is the development of an innovative TIG robotic welding torch with an adaptive changing system that can easily enable a reliable changing of TIG welding torch heads. This leads to achieving the following technical advantages:

- Provide the simplicity of the exchangeable module regard to reproducible fit and interchangeability,
- High positioning accuracy of welding position and wire feed location, and
- Integration of a closed heat transport system – heat dissipation – heat pipe with minimum installation space.

A heat pipe is a component in which the heat can be transported very efficiently from one place to another. The physical effect is used to convert enormously high amounts of energy during the evaporation and condensation of liquids. The characteristics of a heat pipe are the use of evaporation enthalpy, the high heat transfer capacity at low-temperature differences, the effective thermal conductivity, and the diverse geometric design [4, 5]. Within the framework of the flow-thermomechanical - magneto-hydrodynamic (MHD) FE simulation model, the required knowledge of process behavior and its thermo-physical – flow-mechanical effects for a reliable torch head design are determined. This allowed to design the torch part geometries that can suit materials, achieve an optimum cooling system of the heat-pipe torch head with a high cooling capacity, and improve the separation between the process media (inert gas, cooling medium) and the welding current. By using FE simulation, a design solution with an optimized physical functional principle for the technical and constructive design of the torch part geometries as well as cooling and the process gas supply is developed and optimized.

FLUID AND THERMO MECHANICAL / MAGNETO-HYDRO-DYNAMIC MODELING TO SIMULATE THE TIG WELDING PROCESS

INPUT DATA FOR PROCESS SIMULATION

The temperature-dependent materials properties (tungsten, copper, and argon gas, etc.) that are used in the simulation process were taken from literature [6-10] or extracted directly from the simulation program library. These were provided as temperature dependent functions for the software calculations. The electrical and thermal conductivity of the gas was further extended as a Gaussian function with a normal distribution and implemented in the model data. Pure argon was used as the shielding gas. The following material data was also used:

- Density,
- Specific heat capacity, enthalpy,
- dynamic viscosity,
- Thermal and electrical conductivity,
- Emitted radiation: net emission model,
- Radiation properties and heat transfer coefficient,
- Binary diffusion coefficient.

The torch part geometries that are required for the model were extracted from a previously developed CAD model. With this model, the finite element network model was integrated for all model domains and interfaces. The necessary welding data were determined using experimental investigations and then integrated into the FE model.

MODEL DEVELOPMENT – MODEL DETAILS

By means of mathematical and numerical modeling of thermophysical, fluid mechanical process sequences in TIG arc welding, a detailed process analysis to capture and describe the heat balance and the resulting thermophysical effects of the TIG welding process can be performed. The resulting process knowledge makes it possible to develop a fundamental understanding of the processes involved taking into account the TIG process characteristics. This understanding enables for the efficient technical development and design of a functioning TIG welding torch. An exact knowledge of the processes in the TIG arc and a detailed description of the energy flow into the torch environment greatly contribute to a load adapted torch design and a faultless construction. The modeling of the arc was performed with the aid of the magneto hydro dynamic (MHD) equation system. This is understood as a combination of the conservation equations of mass, impulse and energy from fluid mechanics with the Maxwell equations of electromagnetics. The used Maxwell equations are shown below.

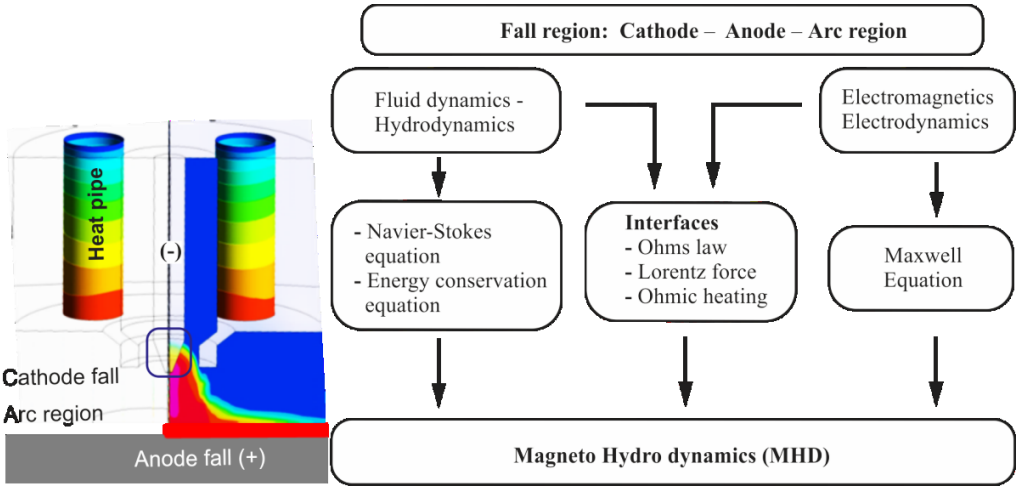

Fig. 1 TIG arc – MHD model

In the MHD, the electrical and magnetic properties of the liquid are described by the electrical conductivity (γ) and the magnetic permeability (μ_o) respectively. Mostly external electrical field and the shielding gas flowing through the magnetic field, which allows the current to flow. The magnetic field results from the superposition of external and self-generated fields. The fundamental equations of electromagnetism are the Maxwell equations. It is used in the MHD model to calculate the electric current density and the magnetic field. For a stationary discharge, the preservation formula is valid, taking into account the quasi-neutrality [8-12]:

$$div\ \vec{j} = 0 \tag{1}$$

The current density follows from the generalized Ohms law. The induced field strengths and the Hall field are negligible compared to the field strength in the TIG arc. Thus Ohm's law applies as:

$$\vec{j} = -\gamma\ grad\,\Phi + \vec{j}_B \tag{2}$$

The magnetic potential $(\vec{A})$ is described by permeability (μ_0) and current density $(\vec{j})$:

$$div\,(grad\ \vec{A}) = -\mu_0 \cdot \vec{j} \tag{3}$$

and the magnetic field can be calculated with:

$$\vec{B} = rot\ \vec{A}$$
$$\vec{B} = \vec{B}_0 + \vec{B}_I \tag{4}$$

The simulation of the arc welding process can thus be carried out by the coupling of computational fluid dynamics with the other physical effects, in particular, the coupling of the individual electromagnetic effects such as electric charges, magnetic dipoles, electromagnetic fields, and forces. In the case of hydrodynamics and electromagnetism, the current that flows through a flowing conductive fluid is formulated as follows:

$$\vec{j}_B = \gamma \, \vec{u} \; x \; \vec{B} \tag{5}$$

In a TIG arc, the electric gas discharge takes place as a result of the sufficiently large electric potential between the cathode (tungsten electrode) and the anode (workpiece), then the electric current flows through a partially thermally ionized gas. Due to the high electrical current density and resistance heating, the necessary temperature to maintain the arc is generated. The limitation of the conductive cross-section of the TIG arc stabilizes the resulting gas discharge. The electrical gas discharges can be divided into three characteristic voltage-drop ranges. These voltage-drop ranges are the cathode and anode drop ranges as well as the voltage drop across the arc region. In contrast to the arc range, the transitions of the arc range to the anode or cathode (drop ranges) cannot be described with LTG boundary conditions. This is due to the too low plasma temperature in this range. At the interface between the arc and the electrodes, the gas temperature is less than 7000 K. Thus, assuming LTG characteristics, the electrical conductivity is too low for the carrier transport to be realized. Instead, the mechanisms of charge carrier transport is characterized by electron and ion diffusion, which are influenced by electron emission at the cathode as well as recombination effects of the charge carriers. Modeling of these effects is very complex, and it can be realized through the consideration of electron diffusion due to ambipolar diffusion, or during the magnification of the grid elements on the electrode. In the drop ranges, the model of Lowke and Sansonnes [15] is used, which is based on the comprehensive simulation of effects in the arc and drop ranges. This allows for the TIG welding process to have self-consistent physical modeling of the arc approach and the energy input to the electrode. The diffusion of electrons is considered using a general electron transport equation (6). This includes the ambipolar diffusion, the term considering recombination, the electron drift (ϖ) and the cathode as an electron source and the anode as an electron sink. The model is based on the electron balance equation:

$$\frac{\partial N_e}{\partial t} = div \, D_a \, grad \, D_e \, (N_0 \, G - N_e^2) + \alpha \varpi N_e + S_e \tag{6}$$

where (N_e) is the electron number density, (D_a) the ambipolar diffusion coefficient, (D_e) the electron-ion recombination coefficient, and (N_0) the neutral atom number density according to [15]. The thermal ionization term (G) = $(N_e)^2 / N_0$ is defined by the diffusion model and in this equation N represents the given density (N). The current flow is defined by the electrical conductivity (γ_e) of the electrons and the electron diffusion (Φ). In order to avoid zero values for the number of electrons at the anode surface, the electron absorption rate was defined as $N_e = D_e N_e / \lambda_m$, with ($D_e$) as the electron diffusion coefficient, and (λ_m)

as the diffusion wavelength. For the conservation equation of the electric current, the following Poisson equation was used:

$$\sigma grad\ \Phi = eD_e\ grad\, N_e \tag{7}$$

Thus, resulting from [15] a higher electrical conductivity with an increase of the electron concentration in the near-electrode regions is given in the following:

$$\gamma = en_e\,\mu_e = \frac{e^2 n^2}{m_e\,\upsilon_{th}(n_i\,AQ_{ei} + n_0\,BQ_{e0})} \tag{8}$$

The representative electron concentration at the cathode is calculated through the flow of electrons, the product of the unit charge, and the electrons thermal velocity. The electron flow is calculated by the Richardson equation for doped tungsten electrodes. The energy input to the cathode (S_{Hc}) is derived from the sum of the heating by impacting ions (S_{Hi}), the cooling by the emitted electrons (S_{He}) and the radiation emission rate.

$$S_{HC} = S_{Hi} + S_{He} - \varepsilon\delta_{SB}T_k^4 \tag{9}$$

With:

$$S_{He} = j_e\Phi_w \tag{10}$$

$$S_{Hi} = j_i(U_{i\,-}\,\Phi_w) \tag{11}$$

$$j_i = j_i(j_{ges\,-}\,j_i) \tag{12}$$

The calculation of the electron current density is based on the Richardson's equation for thermal emission. The work function of a doped tungsten electrode (La_2O_3), according to [15] has to be considered in the heat sink. The doping of the tungsten electrode increases the number of emitted electrons. For the cathode and anode constant radiation emission factors, a ($\varepsilon = 0.5$) are considered. At the anode, the charge carrier transport takes place with electrons. This applies to the input energy in the anode surface (workpiece):

$$S_{HA} = j_{\Phi\,A} - \varepsilon\delta_{SB}T_k^4 \tag{13}$$

The calculation of heat transfer at the electrodes is carried out by the flow solver incorporated in ANSYS CFX. As shielding gas for the TIG welding, pure argon is used. Furthermore, the material properties calculated in [6-10, 13-17], and net emission coefficient of the radiation is used. By implementing a diffusion model, it is possible to calculate the temperature field and pressure gradients. According to the MHD model, the basic equations of fluid dynamics, the Navier-Stokes equations, are to be used for the

numerical simulation. These equations embody a system of nonlinear partial differential equations of 2nd order, consisting of mass conservation, impulse conservation, and energy conservation equations. From Newton's second law the conservation of momentum is derived. The temporal change of impulse is equal to the sum of the forces acting on the volume element.

$$\frac{\partial(\vec{u})}{\partial t} + \vec{u} \cdot grad(\vec{u}) = -\frac{1}{\rho} grad(\vec{\rho}) + \frac{\eta}{\rho} \Delta(\vec{u}) + \vec{f}_S \tag{14}$$

Furthermore, (t) represents the time, ($\vec{u}$) the velocity vector, (η) diffusion coefficient, (ρ) the pressure and ($\vec{f}_S$) the force vectors in the individual TIG arc region. The individual forces in the arc region can be described through the Cartesian coordinate system and in the equation terms. These forces include the force resulting from the pressure gradient, the frictional force due to shear forces, and the body force. The Lorentz force is implemented using the MHD model and thus applies:

$$\vec{f}_L = \vec{J} \; x \; \vec{B} \tag{15}$$

Here the vectorial quantities are the electric current density and the magnetic field. The heat transfer to the outside is carried out by heat conduction. The enthalpy equation from the first law of thermodynamics describes the heat transfer in an open system with a slowly flowing fluid:

$$\frac{\partial H}{\partial t} + div(\rho \cdot H \cdot \vec{u}) = div(\kappa \cdot grad(T)) + \frac{\partial \rho}{\partial t} - S_{rad} + S_h \tag{16}$$

Where (H) is the enthalpy, (t) the time, (T) the temperature, (ρ) the density, ($\vec{u}$) the vector of the velocity components, (κ) the thermal conductivity and (S_{rad}, S_h) the resistance heating in the radial and vertical directions. Here, the net emission of radiation and the resistance heating are taken into account. In the arc phase, the electromagnetics with applied voltage and current is produced through an imposed electric potential, a magnetic field, the Lorentz force, and resistance heating. The resistance heating is the main heating mechanism of the arc region, while the major cooling mechanism is radiation. The Lorentz-force is responsible for a reduction of the arc region volume and thereby an increase in velocity and pressure in the arc region axis.

In summary, it can be said that these physical effects occur in the TIG arc region, the material melting region, and the current flow region. Their magnitude and intensity depend mostly on TIG welding parameters and arc composition in the cathode region. By using the magneto-hydro-dynamic calculation model, taken into account the drop region mechanisms, as well as the TIG arc and its physical effects. The TIG arc and its physical effects can be described in detail by using the aforementioned equations. In addition to the implementation of the additional equations, also the grid to adapt this model approach is

required. In this case to gradient of the electrons correct mapping concentration, very fine grid resolution is necessary.

MODEL GEOMETRY FORMATION – DEFNITION OF PROCESS CONSTRAINTS

Figure 2 shows the developed, procedural FE-simulation model based on the created CAD model. Due to the symmetry of the design, only half of the geometry of the torch head was modeled. The FE-model geometries and domains were developed using hexahedral 3D node elements and a fine FE mesh, as seen in Figure 2. This geometry includes the torch base body, the electrode as a cathode, gas nozzle for shield gas supply, Heat pipe area – domain for cooling, the workpiece as the anode, and the flow regions of shield gas and the arc area, as shown in Figure 2a-c.

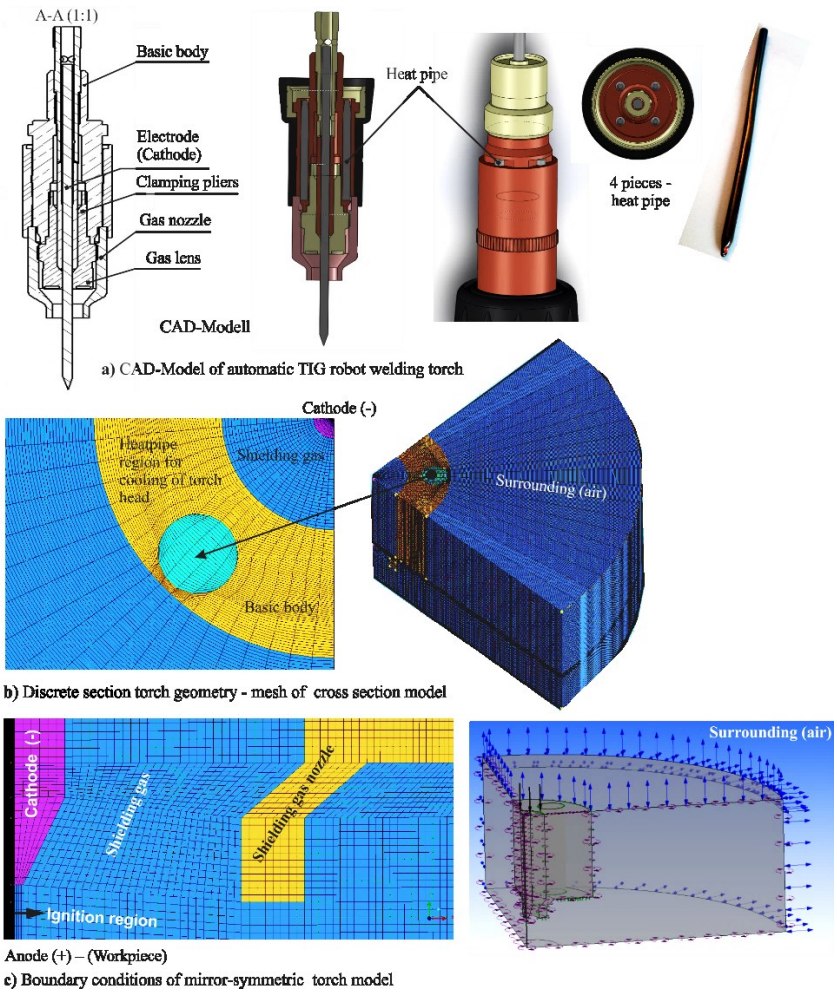

Fig. 2 Meshed model of the axially symmetric torch construction and definition of process boundary conditions

The required temperature-dependent material properties and the welding parameters were provided and incorporated into the FE-model. The selected materials were tungsten for the electrode, copper for the main body as well as, the heat pipe – region, and pure argon as a shielding gas. Overall, an axially symmetric, thermal fluidic simulation model was developed, in which the heavily stressed torch parts were meshed with a higher density. With the higher mesh density, it was possible to overcome the difficulties that arise from the high temperature, arc pressure, and flow velocity. Distribution gradients in those regions under high stress and strong nonlinearities that arise from the temperature-dependent material properties and predefined thermal boundary condition and conduction condition, i.e. (thermal radiation, convection, junction, and flowing gas) that are defined by the FE-model.

With the completion of the meshing of the modeled torch head and the definition of temperature dependent material properties, the characteristics of the torch part geometry and process media such as gases and air and the contact surfaces of the FE model were set to the defined fluids and integrated at the participating torch geometry surfaces. The defined interfaces between the solid areas and the contacted fluids were defined by adiabatic boundary conditions. It is further determined that the shielding gas flows in the gas nozzle at a constant flow rate, which is a linear function of time. Under the use of mathematical equations (which are described above in detail), the information that necessary for the FE-model thermal boundary and transition conditions are defined for the TIG welding process and then incorporated into the model. These boundary conditions include thermal radiation, thermal conduction, heat transfer through heat pipe (cooling of the torch head), the process gas, and the surrounding air. The arc ignition took place under the action of the current flow and the shielding gas (argon) at temperatures above ~7000 K is partially ionized. At this temperature, the discharge process takes place and starts the argon gas partially to ionize. Due to the thermal effect of the temperature, the gas is partially ionized and extended, depending on their ionization energy. On the basis of an artificial energy that is defined by the manipulation of the electrical conductivity, over a Gaussian bell curve with an exponential function in a defined local coordinate system, within the region between the cathode and the anode, the required gas partially ionization temperature was reached at about ~ 7000 K for ignition of the arc. From the arc properties advantage, radiation levels have been formulated as a temperature dependent net emission within the mathematical model. This allows solving the, already described, MHD equation system for the existing temperature and flow distributions in the arc, cathode, and workpiece area within the structured FE model.

Furthermore, it is necessary for the energy conservation, to define interfaces, constraints in terms of flowing gas, electric charges and their potential, and the magnetic field and the vector potential. Thus, the resulting heat transfer is based on the defined processes. In addition, the device constraints can be determined. The outer boundary conditions shown in Table 1 were used for the TIG welding – FE model. To avoid collisions of the gas particles with the geometry surfaces at the gas flow region also to avoid a more rapid drop in temperature in the region of the base body, the process starting temperature is set to T = 300 K and a modeling of process and material-dependent temperature transfer from the solid body to its surrounding was performed. Using the defined material and process constraints and the necessary mechanisms for the shielding gas flow, the drop ranges of cathode, anode, arc region, and heat distribution for the shown FE model were modeled

procedurally and integrated iteratively. With a defined maximum torch electrical performance (I = 200 A) extensive transient FE-simulations were conducted, and taking into account the:

- Temperature-dependent material properties of auxiliary and torch materials,
- Current density and the electric potential (welding current and voltage)
- Shielding gas flow and its effects,
- Heat transfer to the torch part geometries and cooling effects – heat pipe – heat transfer, predefined boundary and transition conditions.

Table 1: Boundary conditions for the FE Model

Region	Type	T [K]	Process gas / rel. pressure	Current density (j)	Electric potential (ϕ)	Magnetic potential
Inlet – Fluid shielding gas	Inlet	300	$\dot{m}_{SG}$ * P	$\frac{\partial \phi}{\partial n} = 0$		$\frac{\partial A_x}{\partial n} = \frac{\partial A_y}{\partial n} = \frac{\partial A_z}{\partial n} = 0$
Inlet – Cooling heat pipe	Inlet	300	-	-		$\frac{\partial A_x}{\partial n} = \frac{\partial A_y}{\partial n} = \frac{\partial A_z}{\partial n} = 0$
Shielding gas nozzle Top	Wall	300	0	-		$\frac{\partial A_x}{\partial n} = \frac{\partial A_y}{\partial n} = \frac{\partial A_z}{\partial n} = 0$
Cathode – Section	Section	300	-	j		$\frac{\partial A_x}{\partial n} = \frac{\partial A_y}{\partial n} = \frac{\partial A_z}{\partial n} = 0$
Fluid – Cathode	Interface	flux	-	flux		flux
Fluid – Shielding gas nozzle	Interface	flux	-	$\frac{\partial \phi}{\partial n} = 0$		flux
Fluid – Workpiece	Interface	flux	-	flux		flux
Opening atmosphere	opening	300	P0	-		0
Workpiece – Bottom	Interface	$\frac{\partial T}{\partial n} = 0$	0	0		$\frac{\partial A_x}{\partial n} = \frac{\partial A_y}{\partial n} = \frac{\partial A_z}{\partial n} = 0$
Workpiece – Wall	Wall	300 K	0	ϕ_S		$A_x = A_y = A_z = 0$

The technical and design suggestions for the torch parts design with respect to the cooling, shield gas supply, and the construction of a functional TIG welding torch, a prototype was derived and iteratively optimized. In this case, the possible thermomechanical loads on the torch functional parts under the influence of the gas flow, the current density, the electric potential and the arc pressure due to the electromagnetic effect were determined. As a basis for the simulation, the following geometric parameters and geometrical structure were defined:

- electrode diameter: d_E = 2.4 mm,
- electrode grinding angles: α_E = 20 °,
- 4 x heat pipe diameter: d_P = 2.6 x 60 mm,
- gas nozzle – bowed pipe diameter: d_P = 8.50 – 14.0 mm.

FE CALCULATION RESULTS

CURRENT DENSITY, ELECTRICAL POTENTIAL, TEMPERATURE FIELD DISTRIBUTION, ARC PRESSURE, SHIELD GAS FLOW AND PARTICLE VELOCITY

Under the defined TIG welding process boundary conditions and by using the thermo-mechanical / magneto-hydrodynamic FE model, the temperature distributions and their resulting physical effects in the TIG arc area and the torch parts were determined and analyzed. The individual images in Figure 3 show the distribution of the calculated arc and gas nozzle temperatures, the current density, the arc pressure, and the resulting temperatures at the torch cooling system – heat pipe and the flow velocity. The calculations were carried out using process parameters of I = 100 A, shielding gas flow rate= 12 l min^{-1} under the influence of the torch cooling system (heat pipe). It was noticeable that the calculated maximum arc temperature T = 17330 K on the arc axis is directly below the tungsten cathode. At the area of the gas nozzle, the arc cross-section is expanded so that a typical open TIG arc bell is formed. This expands rapidly below the nozzle, which leads to a high heat flow within the anode area. The Lorenz force is the cause of an arc flow that determines the dynamic pressure at the workpiece surface. Consequently, the reduction of the arc pressure is caused due to increasing the thermal gas conductivity. It can also be seen that the maximum calculated temperature at the lower edge of the gas nozzle was T = 320 K, which corresponds well to the defined conditions for the torch cooling. This result guarantees a stable welding process under the defined torch cooling system – heat pipe tube.

Furthermore, Figure 3 shows the calculation results of the distribution and intensity of the current density, the arc pressure (dynamic pressure), and the flow velocity of the particles within the arc and the anode area (workpiece). Here the discharge regions are different in temperature, velocity, and potential gradients. In the area of the nozzle, the arc is characterized by a relatively high voltage fall and a high mean temperature of 17330 K. A maximum flow velocity of $\nu = 200$ m s^{-1} at the arc core was determined. The high outflow velocity from the nozzle is due to the associated thermal gas expansion and continuity conditions of the mass flow. However, the maximum speed is calculated under the gas nozzle in the area of the arc axis. This is due to the Lorentz force of the electromagnetic field, which cause arc projection at the cathode and it is to be regarded, as the dominant cause for the suction of external shielding gas directly under the gas nozzle. This effect causes an increase in velocity that leads to arc expansion under the gas nozzle.

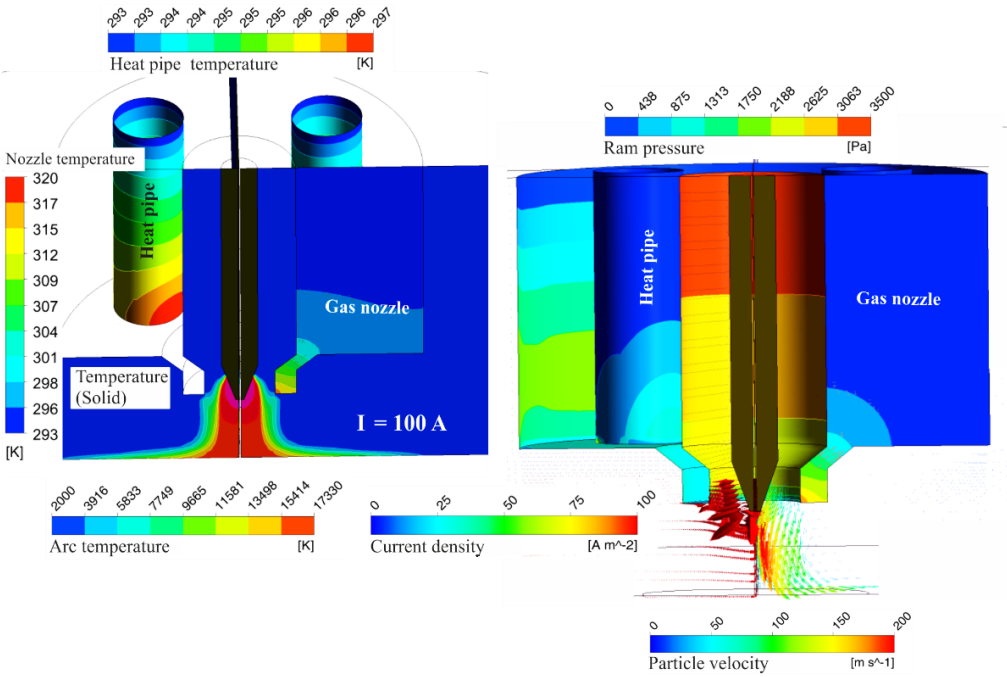

Fig. 3 Calculation results: TIG arc temperature, current density, ram pressure and flow particle velocity

VERFICATION OF FE MODEL BY PRACTICAL EXPERIMENTS

For an optimal technical-constructive design of the heat pipe cooling system in the torch head, temperature measurements were carried out to determine the heat dissipation at the heat pipe as shown in Figure 5a. Using the test system (thermocouples attached to the heat pipe with a control device) as shown in Figure 5a, the measured temperatures show that the heat generated flows error-free from the hot areas to the colder areas. The flow rate depends on the pipe cross-section as well as pipe material thermal coefficient of conductivity. Thus, the technical function ability of the heat pipe was clearly demonstrated.

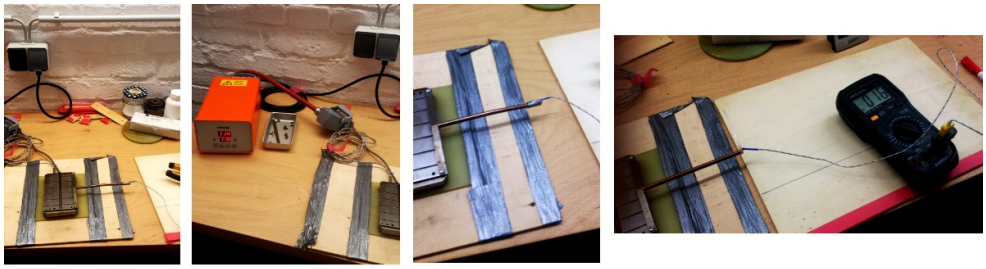

a) Direct measurement of heat dissipation through heat pipe

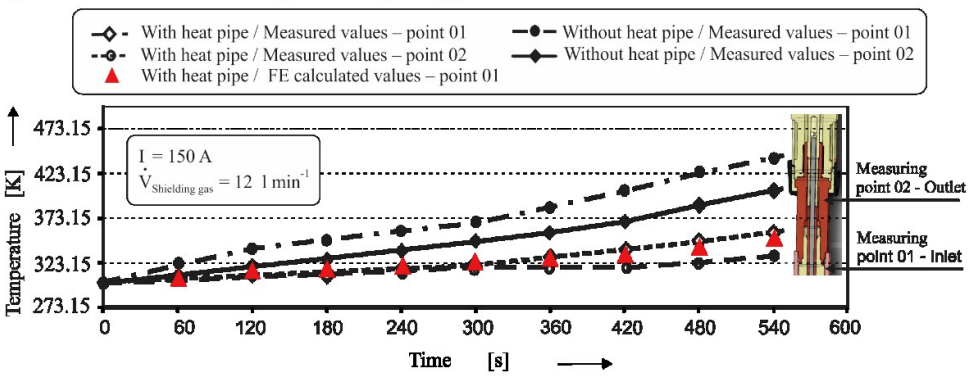

b) Measurement results of heat dissipation through heat pipe during TIG welding process

Fig. 4 Comparison of the calculated and measured of heat pipe temperatures during the welding process by means of attached thermocouples

Furthermore, with and without the heat pipe, under the predefined welding parameters (welding current value: I = 150 A, shielding gas: 12 l min^{-1}), the thermal and fluid mechanical influencing variables of cooling effects in the torch head up to a welding time of 540 seconds were examined, see Figure 5b. Thermocouples were installed on the outer surfaces of the torch's head gas-nozzle, also in the cooling parts of the heat pipe that are attached to the torch head. The results were applied for verification of the FE simulation model and verification of the heat pipe function during the welding process. The torch's head temperature measurements without heat pipe tubes show the larger difference compared to the temperature measurement by using heat pipe cooling. It is noticeable here that higher temperatures were recorded without the heat pipe. Especially at the lower edge of the gas nozzle, the temperature reached up to 438.15 K, while the measured temperatures with heat pipe are less than 361.15 K. Furthermore, the measured temperatures agreed with the simulation results. The maximum temperature measured at the gas nozzle – lower edge of the "highly loaded temperature range" was 361.15 K, while the maximum FE-calculated temperature is 350.15 K. The difference is < 10 %. Thus, it was shown that the designed heat pipe principle for torch head cooling works technically well and can be considered as optimally for a torch head cooling system. These comparisons also showed the validity of the FE-model and the developed torch concept, as well as the selected materials, are well suited for the design of the torch model and its process-related requirements.

PROCESS PARAMETERS INFLUENCE – INVESTIGATION TO OPTIMIZE THE TORCH COOLING AND GAS SYSTEM

To determine the influence of the variation of the welding current and shielding gas quantity on the cooling system efficiency, FE-calculations were performed for the torch including torch-cooling system – heat pipe. Also, the influence of different welding currents I = 75; 150 A and shielding gas flow rate of = 12 l min^{-1} on the arc formation and its physical attribute were investigated. The simulations and evaluations regarding heat pipe cooled torch, heat dissipation, and flows conditions of the shielding gas were performed. Figures 5 and 6 summarize the influences of the process parameters on the arc formation and its intensity.

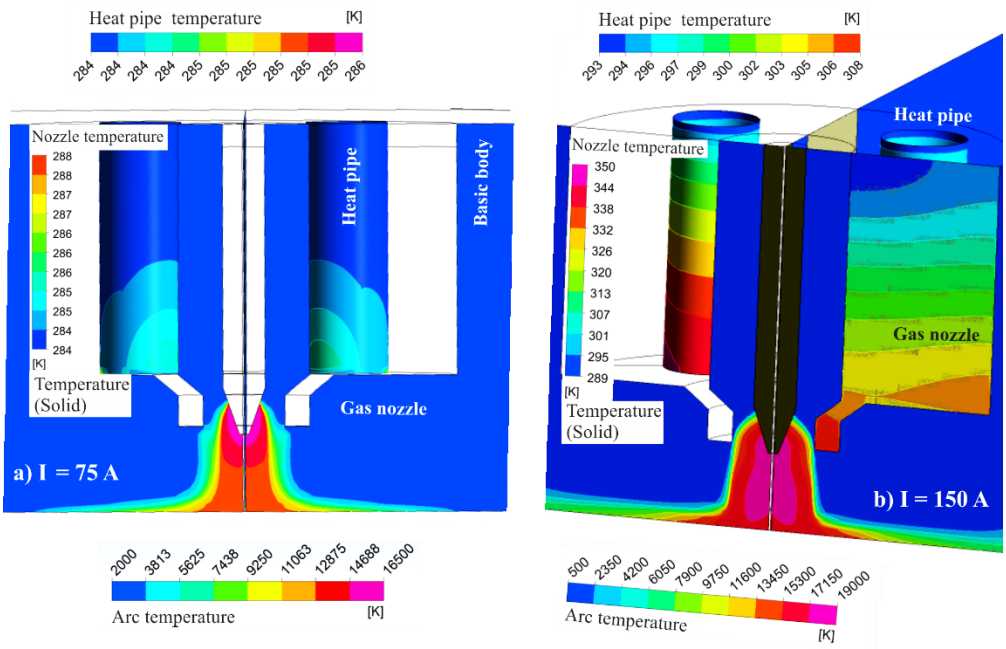

Fig. 5: Calculation results: TIG arc, gas nozzle temperature und heat pipe temperature: **a**) I = 75 A, **b**) I = 150 A; $\dot{V}_{\text{Shielding gas}}$ = 12.0 l min^{-1}

The results of the individual figures 5 and 6 show the calculated temperature distribution in the area of the arc, the gas nozzle, and the heat pipe cooling area. Furthermore, the distribution of the flow velocity of the particles from the arc cross-section to the anode area is shown. This shows that the current fields and particles velocity simulations are functioning well. In addition, results show the protective gas supply is uniform through the torch's head channels and cross-sections.

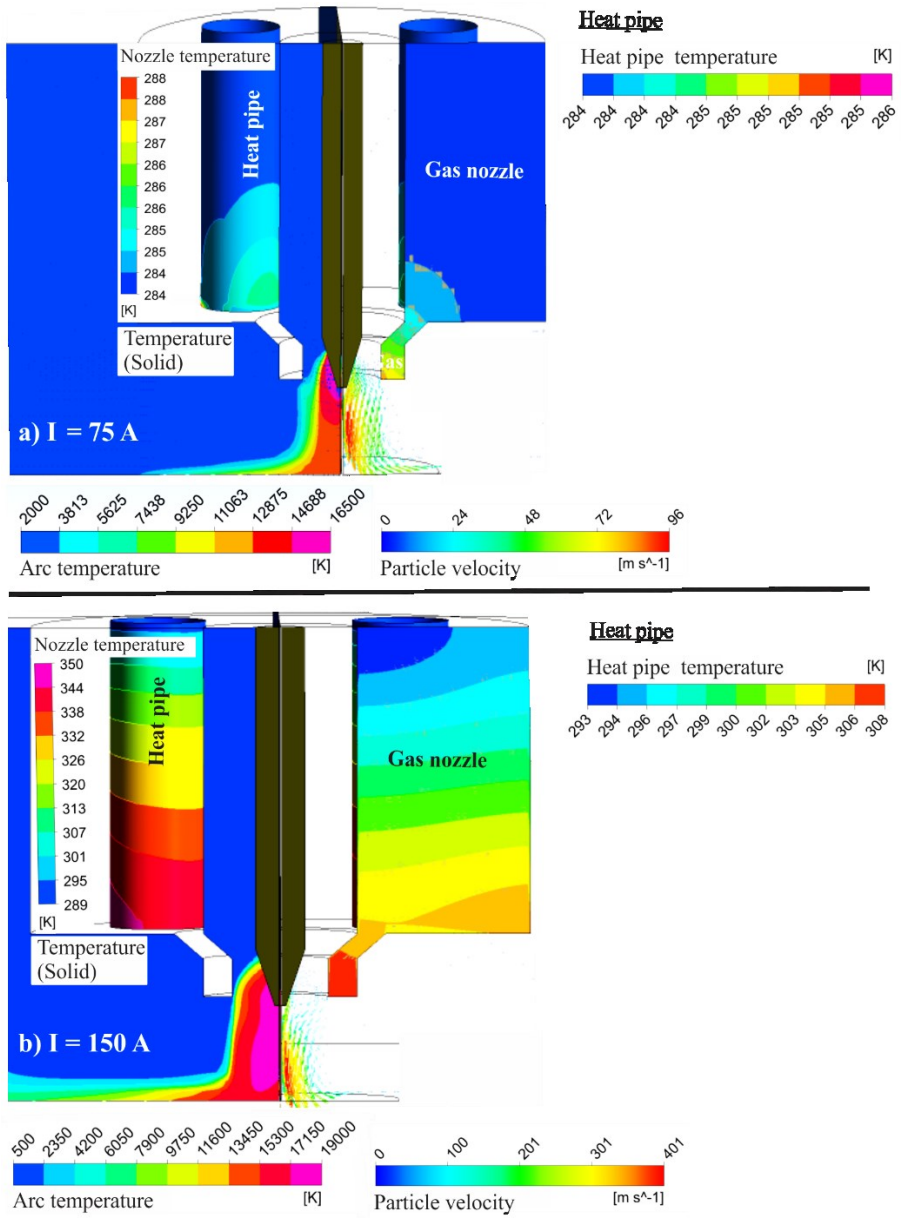

Fig. 6 Calculation Results: TIG arc temperature, nozzle, heat pipe temperature and flow velocity: **a**) I = 75 A, **b**) I = 150 A; $\dot{V}_{\text{Shielding gas}} = 12\ \text{l min}^{-1}$

Furthermore, the calculation results show that the maximum temperatures recorded at the lower edge of the gas nozzle reached up to 350 K. However, at the heat pipe cooling area, the temperature reached up to 308 K at a welding current of I = 150 A. These correspond to temperatures of T = 350 K at the lower edge of the gas nozzle, at the heat pipe cooling area respectively. Thus, the determined parameters fulfill the necessary

cooling capacity for the construction of the automatic robotic-TIG welding torch. Furthermore, the individual images in Figures 5 and 6 show that the temperature of the arc increased from 16500 K to 19000 K as the welding current increased. Increasing of the introduced energy into the arc leads to partial increasing ionization of the shielding gas. As a result, the arc becomes more intense. However, the higher current also leads to a stronger expansion of the TIG arc and therefore leads to a stronger increase of heat radiation in the anode area. At a constant gas flow rate, an increase of electrical potential, current leads to increasing of the arc forces, which increases the magnetic field strength and the arc pressure to P = 7500 Pa and the flow velocity to $\nu = 401$ m s^{-1} at the arc core. The reason for that is an increased degree of ionization of the shielding gas. Due to the temperature increase, the proportion of thermal plasma in the shielding gas area increases during the TIG process, as well as its speed, see Figure 6 and Table 2.

Table 2: Influence of welding current change on arc formation and its physical effects

Current [A]	Max. arc temperature [K]	Max. temperature at the bottom of gas nozzle [K]	Max. temperature at the bottom of heat pipe [K]	Max. arc Pressure [Pa]	Max. flow velocity [m s^{-1}]
75	16500	288	285	2100	96
100	17330	320	297	3500	200
150	19000	350	308	7500	401

The individual images in Figure 6 and Table 2 show the influence of the change in welding current on the behavior and magnitude of the flow velocity and arc pressure. By increasing welding current, the flow velocity, and the arc pressure are rapidly increased. Therefore, a flow rate of $\nu = 401$ m s^{-1} and a maximum pressure of P = 7500 Pa were recorded in the arc core at an increased current of 150 A. When the current increase from 75 A to 150 A, the flow velocity, as well as the arc pressure, increased approximately four times. Based on the simulation results, it is confirmed that the physical arc effects such as arc pressure, current density, electromagnetic fields, and flow velocity increase their intensities were the current is increased. This shows, that in the automated robotic TIG torch, the required reproducibility, interchangeability, positioning accuracy, and faster replacement of torch-head parts, can be realized without errors by using the heat pipe cooling system.

Now, it is possible in automatic-TIG welding torches, which supplied with torch head changing systems to perform welding at higher energy and higher heat input. It is noticeable that the designed cooling principle ‘heat pipe’ for the torch-head cooling system works well. Four heat pipes are sufficient for the predefined torch electrical performance of I = 200 A.

USE OF THE RESULTS FOR CONSTRUCTION OF AN AUTOMATIC TIG ROBOT TORCH WITH HEAT PIPE – COOLING SYSTEM

Figure 7 shows a prototype of the automatic-TIG robot welding torch-head with an exchangeable-head system and heat dissipation (heat pipe tube) torch head cooling system. This prototype was designed according to the defined torch electrical performance of I = 200 A. With this prototype, component joints were welded under realistic working conditions. The evaluation of the torch prototype was carried out through producing welds under various welding conditions using various process parameters. The torch was tested and evaluated for gas tightness and ignition. The ignition process run smoothly and without any problems. Furthermore, by using this welding torch prototype, high-quality welded joints with defined properties can be produced. The welded joints quality shows high reproducibility.

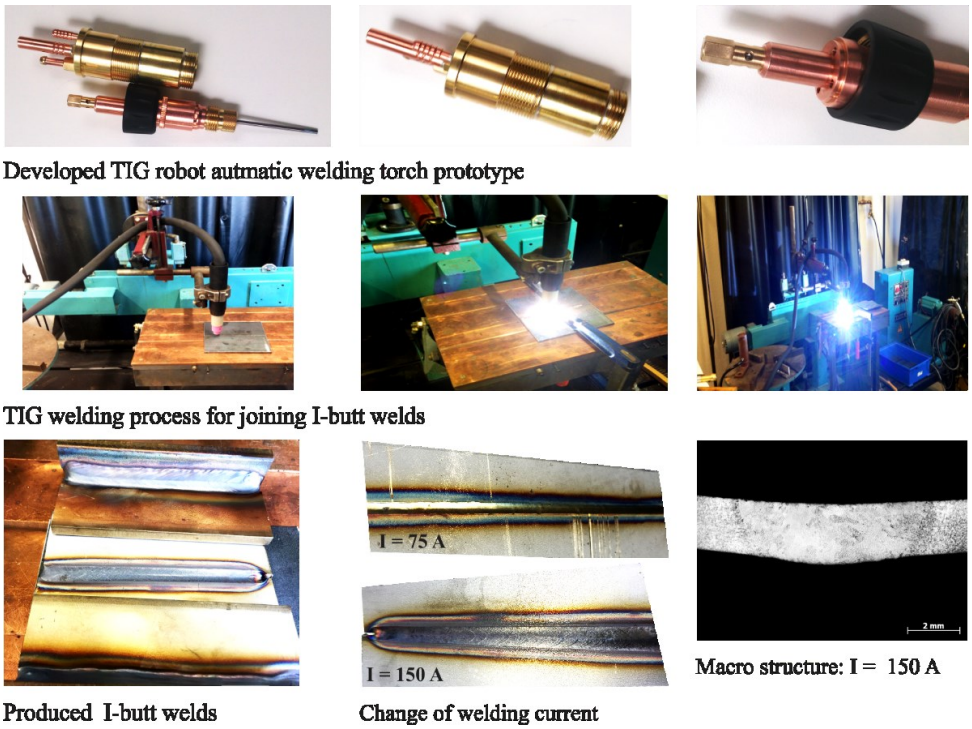

Fig. 7 Developed automatic robotic TIG welding torch prototype

Figure 7 shows the welding tests that were carried out for the torch prototype to produce butt joints using different process parameters. The test results show reproducible, good weld quality, reliable process stability, and easy torch handling. The quality of the welds depends on the process parameters. The performance of the developed automatic robotic TIG-welding torch and its exchangeable head system, as well as its cooling system, was successfully proven.

CONCLUSION FORM THE SIMULATION RESULTS

From the analysis of the simulation results, a new physical operating principle based on the heat dissipation (heat pipe) was derived to design an optimized heat balance for a TIG torch head, which can be used for the design of a functional automatic TIG robotic torch head with its interchangeable head system. The flow-mechanical/MHD model was used to investigate the arc formation and its attribute during automatic TIG robot welding. The physical processes during TIG welding were analyzed and characterized with different process parameters as well as temperature-dependent material properties. Therefore, it was possible to design a torch-head with its defined dimensions, using a heat pipe torch-head cooling system. In addition, the interactions between individual process parameters and the physical effects during the welding process were analyzed, in order to avoid design failures, and creation of a stable, functionally reliable TIG-robotic torch. This leads to the following conclusions:

- Arc characteristic such as formation, intensity, temperature, and flow gas dynamic can be influenced by process parameters.
- The difference between the calculations and the measurements in gas nozzle temperature equal to < 10 %. This indicates the practical application potential of the FE- model.
- The investigated torch cooling system and the gas flow cross-sections corresponded to the defined torch head design.
- The suitability of the construction of the automatic-robotic TIG welding torch including its exchangeable head system and heat dissipation (heat pipe), was proven through the production of butt joints component.

REFERENCES

[1] H.-J. FAHRENWALDT, V. SCHULER: *Praxiswissen Schweißtechnik, Werkstoffe, Prozesse, Fertigung.* 2. überarbeitete und erweiterte Auflage, Springer Vieweg, Wiesbaden, 2009. – ISBN: 978-3-87155-970-9.

[2] K.-J. MATTHES, W. SCHNEIDER: *'Schweißen von metallischen Konstruktionswerkstoffen'*, 5.; neu bearbeitete Auflage Fachbuchverlag Leipzig in Carl Hanser Verlag, München, 2012. – ISBN: 978-3-446-42073-1.

[3] J. P: SCHULZ: *TIG-Process with dual shield Intermediate process between TIG and plasma arc welding*, *Wdg. In World, 24* (1986), H. 11/12, pp. 248/58.

[4] A. BEJAN, D. A. KRAUS: *Heat Transfer Handbook*. Wiley & Sons, Hoboken NJ 2003, ISBN 0-471-39015-1.

[5] T.P. GOTTER: *Principles and Prospects of Micro Heat Pipes, Proc*. *5th Int. Heat Pipe Conf, Tsukuba, 1984* – Japan Technology & Economics Center Inc., Vol. 1.

[6] Y. S. TOULOUKIAN: '*Thermophysical Properties of Matter (14 vol.)*', New York, 1979 ff.

[7] Committee AIH. ASM International v2, '*Properties and selection-nonferrous alloys and special-purpose materials',* 10th ed. OH: metals park 1990. – ISBN 0-87170-378-5.

[8] K. ALALUSS**:** '*Modelbildung und Simulation des Plasma-Schweißens zur Entwicklung innovativer Schweißbrenner – Modeling and simulation of plasma welding for the development of innovative welding torches*', Habilitation, Technische Unversität Chemnitz 2017.

[9] K. ALALUSS, G. BÜRKNER, P. MAYR**:** *Process simulation of plasma-arc welding for the development of an orbital plasma arc welding torch*, 11th International Seminar Numerical Analysis of Weldability, Mathematical Modelling of Welding Phenomena 11 (2016), pp. 23/42, printed bound Styria Print GmbH, Gratkorn, Austria 2016, – ISBN 978-3-85125-490-7.

[10] K. ALALUSS, G. BÜRKNER, P. MAYR**:** *Simulation of micro-plasma powder deposition for advanced welding torch design*, 10th International Seminar Numerical Analysis of Weldability, Mathematical Modelling of Welding Phenomena 10, Graz – Seggau, pp. 705 - 722, printed bound Styria Print GmbH, Gratkorn, Austria 2013. – ISBN 978-3-85125-293-4.

[11] M. SCHNICK, M., U. FÜSSEL, J. ZSCHETZSCE: *Strömungsmessung und Simulation von Lichtbogen- und Plasmaprozessen.*, Aachen, GST 2006.

[12] S. ROSE, U. FÜSSEL, M. SCHNICK: '*Modellierung des dynamischen Lichtbogenverhaltens unter Nutzung experimenteller Daten*'. DVS-Berichte Band 275. S. 545 – 553, DVS-Verlag, Düsseldorf 2011. – ISBN: 978-3-87155-267-0.

[13] L. SANAONNEN, L.; J. HAIDAR; J. LOWKE: '*Prediction of properties of free burning arcs including effects of ambipolar diffusion*', J. Phys. D: Appl. Phys., Vol. 33, pp. 148 – 157, 2000.

[14] C E MOORE: '*Atomic Energy Levels Circular 467'*, vol 2 (Washington DC: US National Bureau of Standards), 1952.

[15] J. J. LOWKE, M. TANAKA: '*LTE-diffusion approximation for arc calculations* ', J. Phys. D: Appl. Phys. 39 (2006) 3634–3643.

[16] A B MURPHY: '*Diffusion in equilibrium mixtures of ionized gas*', Phys. Rev. E 48**,** 3594 – 3603, 2003.

[17] Lago, F.; Gonzales, J.J.; Freton, P.; Gleizes, A.: *A numerical modelling of an electric arc and its interaction with the anode*: Part 1. The two-dimensional model. Journal of Physics D: Applied Physics, Vol. 37, pp.883-897, 2004.